Growth kinetics of epitaxial Y-stabilized ZrO_2 films deposited on InP

2004 J. Phys.: Condens. Matter 16 8201

(http://iopscience.iop.org/0953-8984/16/46/007)

INSTITUTE OF PHYSICS PUBLISHING JOURNAL OF PHYSICS: CONDENSED MATTER

J. Phys.: Condens. Matter **16** (2004) 8201–8211 PII: S0953-8984(04)84609-5

Growth kinetics of epitaxial Y-stabilized ZrO_2 films deposited on InP

E Vasco[1] **and C Zaldo**

Instituto de Ciencia de Materiales de Madrid, Consejo Superior de Investigaciones Científicas, Cantoblanco, 28049 Madrid, Spain

E-mail: enrique.vasco@epfl.ch

Received 6 August 2004, in final form 18 October 2004
Published 5 November 2004
Online at stacks.iop.org/JPhysCM/16/8201
doi:10.1088/0953-8984/16/46/007

Abstract

The nucleation and growth kinetics of Y-stabilized ZrO_2 (YSZ) films have been studied by atomic force microscopy, scanning electron microscopy and x-ray diffraction. The investigated films are cube-on-cube epitaxially deposited on annealed (100)InP by pulsed laser deposition (PLD) exhibiting a two-dimensional growth habit in spite of the large system misfit ($\approx$13% of tensile strain). Beyond the nucleation regime, the YSZ growth kinetics is analysed within the frame of the dynamic scaling theory. Such an analysis suggests the existence of a unique growth mechanism operating during a wide range of deposition times, i.e., 50–10^4 s. This mechanism corresponds to the diffusion ruled by the surface local curvature and limited by the irreversible aggregation to kinks. On the basis of the achieved results, models accounting for the surface diffusion enhancement induced by PLD are discussed.

1. Introduction

Surface roughness is a relevant issue in most of the micro- and opto-electronic applications of thin films, since it controls scattering processes. For instance, in microelectronic devices, interfacial roughness increases current leakage and reduces carrier mobility through charge scattering [1]; while in waveguides, the optical loss reduction is limited by the optical scattering at rough interfaces [2]. Additionally, the surface roughness hampers the integration of further layers added to the system. Consequently, the understanding of the physical origin of surface roughness in terms of growth mechanisms gathers nowadays an increasing scientific and technological interest. Such an interest multiplies in the case of thin films of dielectric oxides deposited on massive semiconductors, because (i) these oxides are extensively used as buffer

[1] Author to whom any correspondence should be addressed. Present address: Swiss Federal Institute of Technology, Lausanne (EPFL), Ceramic Laboratory, MX-D Ecublens, CH-1015 Lausanne, Switzerland.

layers for the integration of YBaCuO and other functional perovskites [3]; and (ii) since their dielectric constants are higher than those of SiO_2 and Si_3N_4, these materials constitute promising candidates in the scaling down race for nanoelectronics [4].

The study of the surface roughening induced by film growth is often carried out within the framework of the dynamic scaling theory (DST) [5, 6]. This theory allows one to describe the surface evolution by making a comparison of experimental findings with theoretical predictions supplied by continuous and/or discrete (atomic) models [6]. The surface morphology of a growing film (growing surface hereafter) is driven by two types of processes: (i) the kinetic roughening, in which the stochastic fluctuations of the incident flux are redistributed on the growing surface by stabilizing mechanisms [6]; and (ii) the growth instabilities, which are related—for instance—to the mass transport limited by edge-step barriers [7], the non-stochastic incidence of the particle flux (shadowing effect) [8] or to the stress developed during growth [9], etc. While the kinetic roughening mechanisms relax the film surface generating a scale-invariant rough morphology, the destabilizing mechanisms induce additional roughness promoting the development of 3D surface features with mound, pyramidal or columnar shapes [7–9].

The growing surface, $h = h(r, t)$, is characterized by two representative lengths: its roughness $w \equiv [\langle (h - \langle h \rangle)^2 \rangle]^{1/2}$ ($\langle\,\rangle$ denotes spatial average on the film plane) and its lateral correlation length ξ. The scaling approach assumes the roughness of a self-affine (stabilized) growing surface scales with the deposition time t and the system size L as

$$w(L, t) = L^{\alpha} f(t/L^{z}), \tag{1}$$

where $f(x) = x^{\beta}$ for $x \ll 1$ and $f(x) \to$ constant otherwise. This implies that the surface lengths increase with the deposition time, for $t \ll L^{z}$, as $w \sim t^{\beta}$ and $\xi \sim t^{\beta/\alpha} = t^{1/z}$; β, α and $1/z$ being the growth, roughness and coarsening exponents, respectively. Such exponents identify the mechanisms operating during the growth [5, 6] based on the fact that each mechanism originates a characteristic morphological evolution of the growing surface.

In the last decade, an increasing number of works concerning the scaling behaviour of the growing surfaces of vapour deposited films has been performed [10]. Despite this effort, very few of these studies are focused on films prepared by pulsed laser deposition (PLD) and all them have been published in the last six years [11–14]. This fact is surprising since PLD has been extensively used for the preparation of multicationic oxide films [15] (for example, note the progress on high-T_c superconductors, ferroelectrics and magnetoresistors [16]). Furthermore, PLD is especially attractive for the epitaxial growth of dielectric oxides on direct-gap semiconductors regardless of the large misfit between these materials. Thus, cube-on-cube heteroepitaxial growths of CeO_2/GaAs (with a lattice mismatch of 4.5%) [17], CeO_2/InP (8.5%) [18], YSZ/GaAs (9.5%) [19], YSZ/InP (13.4%) [20] and MgO/GaAs (25.5%) [21] have been achieved at moderate deposition temperatures (<873 K). The PLD advantage lies in the fact that the suitable temperatures for the epitaxial growths are somewhat lower than those required in another vapour deposition technique. This temperature difference is crucial for integration with direct-gap semiconductors due to the thermal instability of these substrates [22].

In this paper, we provide new experimental data about the epitaxial growth of Y-stabilized ZrO_2 (YSZ) on InP by PLD, as a prototype of dielectric oxides integrated with direct-gap semiconductors. The study allows us to identify the operating growth mechanisms and their influences on the resulting film morphology, paying special attention to the relaxation of the system misfit stress. In addition to the scaling analysis presented here, some old notions that pointed to an enhancement of the growth kinetics by PLD are discussed in order to shed light on the underlying mechanisms and features inherent in this deposition technique.

2. Experimental procedure

Y-stabilized zirconia ($Zr_{1-x}Y_xO_{2-x/2}$, YSZ) films were deposited on sulfur-doped (100)InP by using a KrF excimer laser ($\lambda = 248$ nm, 16 ns pulses, $\nu = 10$ Hz) focused onto a YSZ ($x = 0.1$) single crystal target (rotating at 20 rpm) at a laser power density of $J = 3$ J cm^{-2}. Substrates were placed opposite to the target at 60 mm, and heated to $T_s = 853 \pm 5$ K during deposition. At deposition temperature, the nominal system misfit becomes[2] $S_0 = (a_{InP} - a_{YSZ})/a_{YSZ} \approx 12.9\%$ ($S_0 = 13.4\%$ at RT). To avoid InP oxidation, YSZ growth was performed in high vacuum ($PO_2 = 8 \times 10^{-7}$ mbar). The roughness of the as-received (100)InP substrate, 0.64 nm, is reduced by annealing down to $w_{InP} = 0.26$ nm. The depositions were performed on annealed substrates. Details of the deposition procedure including the substrate preparation have been reported elsewhere [20]. Under these conditions, YSZ films grew epitaxially with a $\langle 100\rangle\{100\}$YSZ $\parallel$ $\langle 100\rangle\{100\}$InP cube-on-cube orientation at a deposition rate of 0.08 nm s^{-1} in the whole range of deposition times considered, i.e., 2–10^4 s. Note that the deposition conditions required to achieve epitaxial and stoichiometric YSZ films on InP are comprised within narrow windows of values [20]: (i) oxygen pressures higher than 10^{-3} mbar produce a Y-depleted YSZ film; while (ii) deposition temperatures higher than 950 K induce a substrate surface degradation rendered by the P preferential evaporation and/or In reoxidation [22]. On the other hand, (iii) YSZ grows crystalline once the thermal desorption of InP native oxide occurs, which takes place at $T_s > 820$ K in $PO_2 = 10^{-5}$ mbar. The thickness of the films was measured with a Talysurf-50 profilometer and tested by cross-section scanning electron microscopy in cleaved samples.

The film morphology was analysed by scanning electron microscopy (SEM) at very early growth stages and by atomic force microscopy (AFM) in thicker films. The top-view SEM images were taken by means of an ICI DS-130C high-resolution microscope operating at 10 kV. For each sample several AFM images, with sizes ranging from 0.2×0.2 to 10×10 μm^2, were scanned at different sample areas using a Nanoscope IIIa equipment operating in tapping mode with silicon tips (nominal radius ≈ 10 nm). The root mean square surface roughness w_{rms} was calculated from the largest surface area. The power spectral density curves PSD(k), defined as the square of the 2D Fourier transform coefficients of the digitized surface, were provided by the AFM software. The lateral correlation length ξ was calculated from the crossover ($k_c = 1/\xi$) to the saturation of PSD(k) curves. The lattice parameters and crystallinity quality of the films were investigated by x-ray diffraction using a D-500 Siemens diffractometer (with Cu Kα radiation) operating in θ–2θ and rocking curve mode.

3. Results

Figure 1 shows a very early stage of YSZ growth. The annealed (100)InP surface appears decorated by gestation YSZ nuclei, which exhibit a cubic symmetry. Such symmetry is in agreement with the cube-on-cube epitaxial relationship found in thicker films [20]. As the deposition progresses and the nuclei coalesce, a singular morphology emerges, as revealed by figure 2. The 0.8 nm thick YSZ film ($t = 10$ s) exhibits a surface patterned by an orthogonal network (like a square grid) of grooves spreading along the [110]InP and [$\bar{1}$10]InP directions. These grooves, with an average width of 10 nm, isolate surface crystalline areas in a two-dimensional array. As displayed by two typical surface profiles in figures 2(a) and (b), the groove spacing along the spreading directions is around 30–35 nm. The grooves cover $\approx$40% of the film surface. The cubic symmetry of the surface crystalline areas suggests that the

[2] Estimated thermal expansion coefficients at RT: $\alpha_{InP} = 4.5 \times 10^{-6}$ K^{-1} and $\alpha_{YSZ} = 11.4 \times 10^{-6}$ K^{-1}.

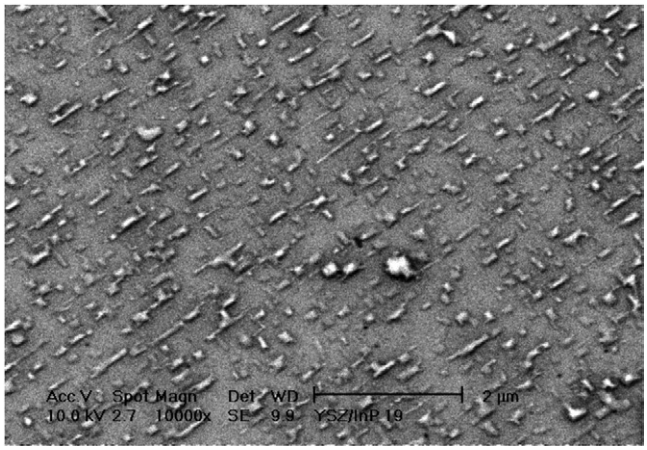

Figure 1. Top-view SEM image of a very early stage (nucleation) of the YSZ growth ($t = 2$ s, coverage ≈ 0.6 monolayer).

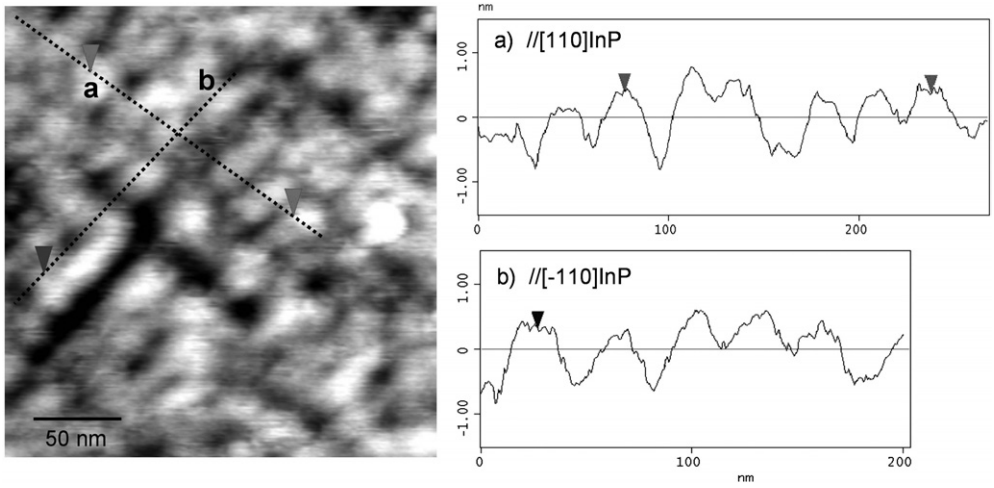

Figure 2. AFM image of the 0.8 nm thick YSZ film ($t = 10$ s). Surface profiles along the [110]InP (a) and [$\bar{1}$10]InP (b) directions.

groove network corresponds to a relaxation mechanism of the system misfit stress connected to the brittle behaviour of YSZ at the deposition temperature used here [23]. This could indicate that the misfit dislocations taking place inside the crystalline areas are insufficient to relieve the system misfit stress. Such dislocations should be spaced less than 5 nm to give rise to a fully relaxed YSZ film. However, for so-high dislocation densities ($>10^{12}$ cm^{-2}, such that the dislocation spacing is of the order of the strained layer thickness), interactions between dislocations become operative, promoting the appearance of new kinetic barriers to the dislocation nucleation [24]. The existence of crystalline areas separated by disordered regions has been previously observed by Bardal *et al* [25] in YSZ films epitaxially grown on SiO_x/(100)Si ($S_0 \approx 5\%$) by transmission electron microscopy (TEM). The fact that these regions, which have been identified in our case as grooves, are periodically distributed for systems with larger mismatches such as YSZ/InP constitutes a new experimental evidence.

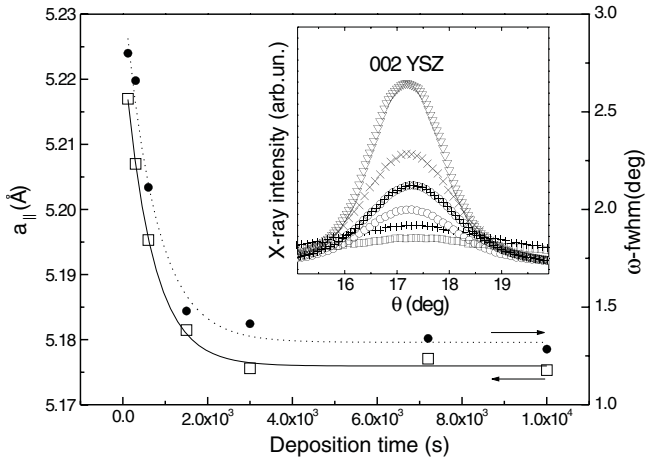

Figure 3. Evolution of the in-plane YSZ parameter (left axis, □) and the full width at half maximum of 200 YSZ rocking curves showed in the inset (right axis, ●) with the deposition time. The curves provide visual help. Inset: the symbols correspond to 300 s (□), 600 s (+), 1500 s (○), 3000 s (⊕), 7200 s (×) and 10 000 s (▽).

The lattice parameters of thicker-than-8 nm YSZ films ($t > 100$ s) have been obtained from 002 YSZ and 113 YSZ x-ray diffractions by using the relationship between Miller indices and the lattice parameters for a tetragonally-distorted cell ($a = b \neq c$). The thickness evolution of the in-plane parameter ($a_{\parallel}$) is displayed in figure 3 (open square). $a_{\parallel}$ decreases as the film thickness increases, revealing a progressive relaxation of the system misfit stress (tensile strain), which includes a thermal contribution imposed upon cooldown to RT. Thus, after a thickness of $h_1 = 10$ nm 95% [$S(h_1)/S_0 \approx 5\%$] of the system misfit stress has been plastically relaxed by means of dislocations and grooves, and after $h_2 = 120$ nm, the film is stress-free [$S(h_2)/S_0 < 1\%$]. By assuming that new grooves are not originated after 10 nm, the thinnest limit of critical thickness (h_c) for the nucleation of misfit dislocation can be computed as $h_c \geqslant [S(h_2) - S(h_1)] \times [S_0(1/h_2 - 1/h_1)]^{-1} \approx 0.5$ nm. Such estimation supports the above-provided hypothesis that points to the fact that the surface crystalline areas are not dislocation-free. A qualitatively similar behaviour to that shown here has been reported by Bardal *et al* [25] for thinner thicknesses such that the there-studied films were not fully relaxed. As the stress relaxation takes place the crystalline quality of the YSZ film, which is evaluated from the full width at half maximum *ω-fwhm* (figure 3, closed circles) of the 002 YSZ rocking curves (figure 3 inset), is progressively improved.

Once the system misfit stress is mostly relaxed (for $t > 100$ s), the YSZ growth kinetics is investigated according to DST as follows. Due to the extreme smoothness of the deposited films, especially for the shortest deposition times, it is necessary to remove the substrate contribution to the system roughness w_{rms} [26] in order to analyse properly the scaling behaviour of the YSZ film roughness. Figure 4 displays the temporal evolution of the corrected roughness $w_{\mathrm{f}} = \sqrt{w_{\mathrm{rms}}^2 - w_{\mathrm{InP}}^2}$ ($w_{\mathrm{InP}} = 0.26$ nm). The YSZ surface roughness increases with the deposition time according to $w_{\mathrm{f}} \propto t^{(\beta=0.22\pm0.04)}$. The so-obtained growth exponent ($\beta < 0.5$) suggests the presence of a stabilizing mechanism relaxing the growing surface laterally [6]. Note that this scaling behaviour is observed for deposition times spanning more than two decades.

The PSD curves of the films grown at different deposition times are shown in figure 5 together with those corresponding to as-received and annealed substrate. The difference

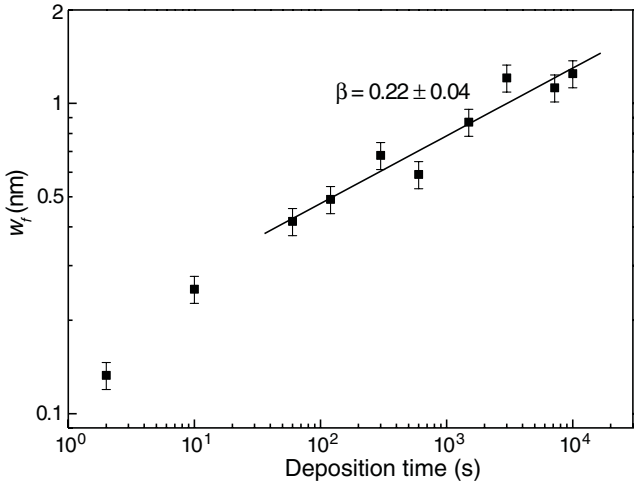

Figure 4. Logarithmic plot of the surface roughness, w_f, versus deposition time for YSZ films grown on annealed (100)InP. The solid line with slope β corresponds to the best fit of the experimental data for $t \geqslant 60$ s.

between the substrate curves for high k values ($k > 2 \times 10^{-2}$ nm^{-1}) points to a short-range smoothing effect (<50 nm) induced by the annealing upon the substrate surface. The film PSD curves show three regions, sorted according to the length scale within the real space: (i) region characterized by a linear log(PSD) versus log(k) dependence for high k values, indicating a strong surface correlation; (ii) saturation region for intermediate k, suggesting that the surface is uncorrelated at these lengths; and (iii) region where film PSD curves reproduce the behaviour of the substrate ones (low k). In the first region, the film PSD curves overlap, exhibiting a common slope $m \approx -4$, which implies a value of the roughness exponent $\alpha \approx 1$ by taking into account that PSD curves of an nD system (here $n = 2$) scales with the spatial frequency k as [27]

$$\mathrm{PSD}(k, t) \propto k^{-n(1+\alpha)} f(k^z t), \tag{2}$$

such that for a correlated surface (with $t \gg k^{-z}$), $f(k^z t) = \text{constant} \Rightarrow \mathrm{PSD}(k) \propto k^{[m=-2(1+\alpha)]}$. The curve overlap in the first region suggests the presence of a single growth mechanism operating in the analysed range of deposition times. Such a mechanism would give rise to a linear increase of the saturated roughness of the YSZ films as the area size inspected by AFM increases (i.e., $w = L^\alpha = L$). A crossover (k_c) separates the first and second region, while the intersections between the film PSD curves and those of the substrate isolate the second region from the third one. The overlap of the PSD curves within the third region indicates that at larger length scale (>500 nm) the film roughness behaviour is determined by substrate surface features. This fact suggests that the revealed growth mechanism operates at shorter lengths.

Figure 6 displays the temporal evolution of the correlation length defined as $\xi = 1/k_c$. ξ spreads with the deposition time following the scaling expression $\xi \propto t^{(1/z=0.26\pm0.02)}$. The coarsening and film surface roughening as the deposition time increases can be qualitatively observed in the AFM images included in figure 6, which correspond to YSZ films deposited during 60 s (inset (a)) and 7200 s (inset (b)).

The scaling coefficients ($\beta \approx 0.22$, $\alpha \approx 1$ and $1/z \approx 0.26$) achieved from the previous analysis agree reasonably with those predicted ($\beta = 0.25$, $\alpha = 1$ and $1/z = 0.25$) by DST for a not very rough growing surface (i.e., $|\nabla h| \ll 1$) evolving under a surface diffusion

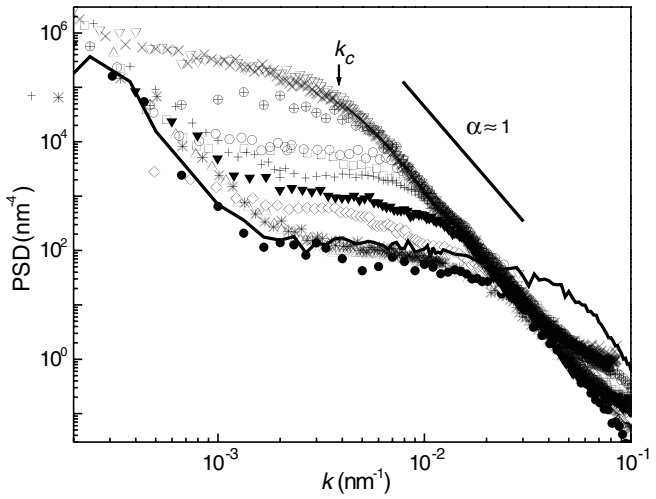

Figure 5. PSD(k) curves of YSZ films grown on annealed (100)InP. The symbols correspond to as-received (solid curve) and prepared substrate (●), 2 s (△), 10 s (∗), 60 s (◇), 120 s (▼), 300 s (□), 600 s (+), 1500 s (○), 3000 s (⊕), 7200 s (×) and 10 000 s (▽). The straight line indicates the slope corresponding to $\alpha = 1$. The crossover k_c of the longest deposition time curve is marked.

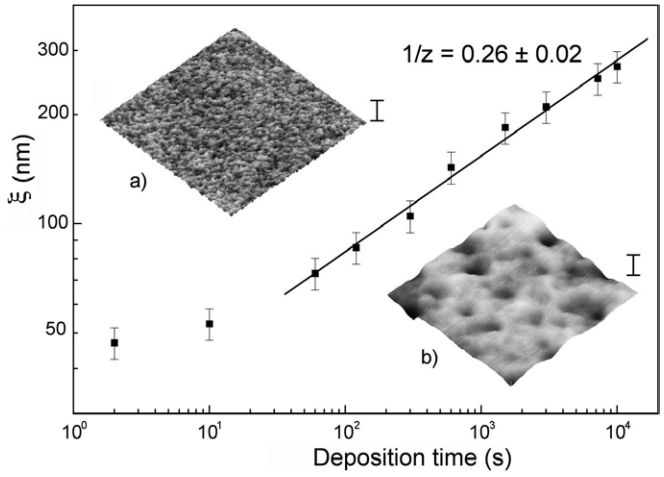

Figure 6. Logarithmic plot of the correlation length, ξ, versus deposition time for YSZ films grown on annealed (100)InP. The solid line with slope $1/z$ corresponds to the best fit of the experimental data for $t \geqslant 60$ s. The insets show AFM images of YSZ films grown at different deposition times: (a) 60 s and (b) 7200 s. The vertical bars indicate 20 nm and the scanned area was $1 \times 1\ \mu m^2$.

mechanism [28]. Such a diffusion mechanism is ruled by the surface local curvature [29] ($\propto -\nabla^4 h$) rather than the surface strain field [9] ($\propto \nabla^2\{S[h(r)]\}^2$), which suggests that the determined correlation lengths are shorter than the crossovers[3] to growth regimes controlled by the misfit strain. In particular, the scaling coefficients obtained here correspond to

[3] The crossover to the stress-controlled growth regime can be estimated as $\sim(\pi\gamma/M)[S(h)]^{-2}$, γ being the surface energy of the stressed YSZ film and M its elastic modulus defined for a cube-on-cube epitaxial film as $M = C_{11} + C_{12} - 2C_{12}^2/C_{11}$ (where C_{11} and C_{12} are components of the elastic stiffness matrix). More details are given in [9].

a low-temperature diffusion limited by the irreversible aggregation to the nearest kinks, which operates within a spatial range where the nonconservative white noise related to random fluctuations of the incident flux prevails [28]. Summarizing, this mechanism would stabilize/relax the growing surface in its dependence on its local curvature by redistributing laterally the stochastic fluctuations of the incident flux at short range [6, 28, 29].

4. Discussion

As pointed out in the previous section, the YSZ scaling behaviour once the misfit stress has been mostly released suggests the existence of a unique growth/scaling regime (spanning a wide range of deposition times) governed by the short-range relaxation of the growing surface through an aggregation-limited diffusion mechanism [28]. This behaviour reveals the predominance of a stabilized 2D Frank–van der Merwe (layer-by-layer) growth mode over 3D growth processes, which is in agreement with the extremely low roughness of the deposited films (e.g., $w = 1.2$ nm in a 800 nm thick film, which implies $w < 0.2\%$ of the film thickness) and the absence of defined surface structures such as grains or column boundaries. The stress relaxation has a crucial influence on the observed growth mode since the equilibrium theories for misfit dislocations [30] predict an upper limit of $S_0 = 7$–8%, which is lower than the YSZ/InP nominal misfit, for the prevalence regime of a layer-by-layer growth. The obtained roughnesses are lower than those found in sputtered ZrO_2 films ($w > 0.8\%$ of film thickness [31]) and those reported for $LiNbO_3$ and $KNbO_3$ oxides grown by MOCVD (typically $w \approx 1\%$ [2]). It should be stressed that the identified diffusion mechanism operates at a deposition to melting temperature ratio as low as $T_s/T_m \approx 0.29$, which corresponds—as predicted by the structure zone model (SZM) [32]—to a regime of diffusion limited by kinetic barriers (probably characterized by 3D growth mode). The key role played by the surface diffusion on the growth of dielectric oxides on semiconductor substrates has been previously observed in the MgO/Si and MgO/GaAs systems [33]. However, the there-reported tendency of MgO to grow with a 3D habit, as expected from SZM ($T_s/T_m \approx 0.25$), suggests the prevalence of kinetic barriers on the growth mode. Such barriers would be likely connected to the deposition technique used (i.e., aerosol-assisted chemical vapour deposition [33]).

If the correlation lengths are interpreted as average diffusion lengths and the completion time of one monolayer ($\tau \approx 3$ s) is taken—in reasonable assumption—as the longest limit of the diffusing species lifetime, a diffusion coefficient $D_s = \xi^2/\tau > 2.4 \times 10^{-10}$ cm^2 s^{-1} for the 800 nm thick film can be estimated. Such an estimation agrees with the values found in other oxides deposited by PLD ($\sim 10^{-10}$–10^{-11} cm^2 s^{-1}) [34, 35]. This diffusion coefficient, that is still lower than those of metals [36] ($\sim 10^{-3}$–10^{-6} cm^2 s^{-1}) and semiconductors [37] ($\sim 10^{-7}$–10^{-14} cm^2 s^{-1}) for similar T_s/T_m ratios, is larger than those obtained in oxides deposited by sputtering and co-evaporation ($\sim 10^{-13}$ cm^2 s^{-1}) [35, 38]. Then, on the basis of the estimated diffusion coefficient and the previously-reported results [39], it can be concluded that the PLD process enhances the growth kinetics of oxide films in comparison with other energetic (e.g., sputtering) or thermal (e.g., evaporation) deposition techniques. These evidences would confirm old notions that pointed to optimal deposition temperatures in PLD somewhat lower than those required by other techniques.

Several models related to the peculiarities of the PLD technique are proposed within the frame of the far-from-equilibrium growth to elucidate the physical origin of the diffusion enhancement. In this context, the outstanding features of PLD are [40]: (i) the pulsed nature of the deposition process having several time constants (e.g., period between pulses ($1/\nu$), pulse width, diffusing specie lifetimes, etc); (ii) the plasma characteristics, i.e., its high ionization degree (up to 70%), supersaturation of energetic particles ($\sim$1–10^2 eV) and reactivity in the

presence of oxygen; (and iii) the plasma-growing surface interaction. An overview of some proposed models is provided below.

(a) Based on the high energies of the ablated light particles ('hot particles'), many works [11, 35, 39] point to a transient mobility of the incident species as the mechanism that accounts for the diffusion enhancement. Hence, the energetic species diffuse over large distances before transferring their excess of kinetic energy to the growing surface. The relaxation path (or thermalization path) would depend on kinetic energy of the incident species as well as on the energy dissipation rate on the growing surface, which is connected to the ability to form bonds mediated by the coupling to the film phonons [41]. In any case, the energy dissipation rates for atomic and molecular species (reactive species) are large enough ($\sim ps^{-1}$ [42]) to reduce the thermalization path to some atomic positions around the landing site [43]. Consequently, it is unrealistic to attribute diffusion lengths of hundreds of nanometres on the highly-corrugated surface (with diffusion barriers $\sim$1.0 eV) of an oxide to a transient mobility mechanism.

(b) Other less extended models support the idea of a diffusion enhancement on a growing surface subjected to a concurrent bombardment by plasma due to the periodic transfer of kinetic energy to diffusing species [44]. The energy so gained by the diffusing species is progressively transferred to the growing surface along their thermalization paths. Unlike the sputtering, such a transfer would be effective for mobile species with lifetimes longer than $1/\nu$. As a result of the periodic nature of this process, a resonant diffusion enhancement under certain deposition conditions—in which the period between pulses matches with the relaxation times of the mobile species—can be expected. Similar resonant phenomena have been previously observed for growths from pulsed fluxes [45].

(c) A third option lies on the diffusion controlled by 'non-reactive' species (i.e., clusters and droplets [12, 46]) weakly bonded to the film surface. Most of them are gestated on the growing surface during the pulse arrival ($\sim\mu s$) due to the plasma supersaturation—as predicted by the classical nucleation theory; see for instance [14, 47]. The kinetics of such clusters would be mainly controlled by the diffusion and the aggregation/dissociation of the smaller species, taking into account that the dissociation rate decreases as the cluster size increases. Another fact to bear in mind is that a decrease of the energy dissipation rate (i.e., larger thermalization paths) for energetic clusters can be expected since the interactions with the growing surface are weakened by the cluster inner bonds [48]. Both pieces of information would point to a diffusion enhancement controlled by the thermalization path of moderate-sized clusters, i.e., large enough to be stable and small enough to be mobile [46]. Note that the massive formation of these energetic clusters on the growing surface (without surface erosion phenomena) is exclusive of PLD because the pulsed nature of the ablation process promotes the quasi-instantaneous cluster nucleation from the supersaturated plasma [14, 47].

Finally, because of the close interrelationship between deposition conditions and plasma characteristics, it is arduous to isolate the influence of the proposed mechanisms by different models on the growth kinetics of the pulsed laser deposited systems. For instance, as the laser energy density increases or the wavelength decreases the supersaturation, the ionization degree and the energy density of the plasma increase concurrently. Thus, a decrease of the surface roughness of Ni and Ti films [49] (YBCO films [50]) has been observed as the laser energy density (laser wavelength) increases (decreases). So, in spite of the proposed mechanisms and points of view argued in this work and others, the nature of the diffusion enhancement induced by PLD, which is responsible for the extremely low roughness observed in several 2D

grown films, continues being a scientific challenge to be clarified. In this sense, new theoretical interpretations as well as TEM investigations are required.

5. Conclusion

In conclusion, the pulsed laser deposition technique can enhance the growth kinetics of Y-stabilized zirconia producing exceptionally smooth and epitaxial films on InP at relatively low temperatures. This stabilized behaviour takes place once the large system misfit stress is mostly released by dislocations and groove nucleation and it is ruled by short-range relaxation of the growing surface via an aggregation-limited diffusion mechanism. Such a mechanism is probably connected to plasma characteristics inherent in the pulsed laser deposition technique.

Acknowledgment

The authors thank L Vázquez for the AFM measurements.

References

[1] Cheng Y C and Sullivan E A 1973 *J. Appl. Phys.* **44** 923
[2] Fork D K, Armani-Leplingard F and Kingston J 1996 *Mater. Res. Soc. Bull.* **21** 53
[3] E.g., superconductors on GaAs: Fork D, Nashimoto K and Geballe T 1992 *Appl. Phys. Lett.* **60** 1621
Manganites on Si: Trtik V, Ferrater C, Sanchez F, Varela M, Fontcuberta J, Bibes M and Martinez B 2000 *J. Cryst. Growth* **209** 842
Ferroelectrics on InP: Vasco E, Vazquez L and Zaldo C 1999 *Appl. Phys.* A **69** S827
[4] Vasco E and Zaldo C 2003 *Mater. Sci. Semicond. Proc.* **5** 183
Forst C J, Ashman C R, Schwarz K and Blochl P E 2004 *Nature* **427** 53
[5] Family F and Vicsek T 1985 *J. Phys. A: Math. Gen.* **18** L75
Family F 1990 *Physica* A **168** 561
[6] Barabási A L and Stanley H E 1995 *Fractal Concepts in Surface Growth* (Cambridge: Cambridge University Press)
[7] Smilauer P and Vvedensky D 1995 *Phys. Rev.* B **52** 14 263
[8] Roland C and Guo H 1991 *Phys. Rev. Lett.* **66** 2104
[9] Srolovitz D J 1989 *Acta Metall.* **37** 621
[10] Deposited by MBE: Tejedor P, Smilauer P, Roberts C and Joyce B A 1999 *Phys. Rev.* B **59** 2341
Sputtering: Lita A E and Sanchez J E 2000 *Phys. Rev.* B **61** 7692
CVD: Ojeda F, Cuerno R, Salvarezza R and Vázquez L 2000 *Phys. Rev. Lett.* **84** 3125
[11] Mayr S G, Moske M, Samwer K, Taylor M E and Atwater H A 1999 *Appl. Phys. Lett.* **75** 4091
[12] Narhe R D, Khandkar M D, Adhi K P, Limaye A V, Sainkar S R and Ogale S B 2001 *Phys. Rev. Lett.* **86** 1570
[13] Durand H A, Nishimoto K and Kataoka I K 2000 *Appl. Surf. Sci.* **154** 387
Vasco E, Zaldo C and Vázquez L 2001 *J. Phys.: Condens. Matter* **13** L663
[14] Combe N and Jensen P 1998 *Phys. Rev.* B **57** 15553
Hinnemann B, Hinrichsen H and Wolf D E 2001 *Phys. Rev. Lett.* **87** 135701
Lam P M, Liu S J and Woo C H 2002 *Phys. Rev.* B **66** 45408
[15] Chrisey D B and Hubler G K (ed) 1994 *Pulsed Laser Deposition of Thin Films* (New York: Wiley) chapters 14–16, 20, 23
[16] Superconductors: Dijkkamp D, Venkatesan T, Xu X D, Shaheen S A, Jisrawi N, Min-Lee Y H, McCean W L and Croft M 1987 *Appl. Phys. Lett.* **51** 619
Ferroelectrics: Horwitz J S, Grabowski K S, Chrisey D B and Leuchtner R E 1991 *Appl. Phys. Lett.* **59** 1565
Magnetoresistors: Von Helmot R, Wecker J, Holzapfel B, Schultz L and Samwer K 1994 *Phys. Rev. Lett.* **71** 2331
[17] Nagata H, Yoshimoto M and Koinuma H 1992 *J. Cryst. Growth* **118** 299
[18] Norton D P, Pearton S J, Christen H M and Budai J D 2002 *Appl. Phys. Lett.* **80** 106
[19] Tiwari P, Sharan S and Narayan J 1991 *Appl. Phys. Lett.* **59** 357
[20] Vasco E, Vázquez L, Aguiló M and Zaldo C 2000 *J. Cryst. Growth* **209** 883

[21] Nashimoto K, Fork D and Geballe T 1991 *Appl. Phys. Lett.* **60** 1199
Tarsa E J, De Graef M, Clarke D R, Gossard A C and Speck J S 1993 *J. Appl. Phys.* **73** 3276
[22] Farrow R F C 1974 *J. Phys. D: Appl. Phys.* **7** L121
Hollinger G, Bergignat E, Joseph J and Robach Y 1985 *J. Vac. Sci. Technol.* A **3** 2082
[23] The brittle-to-ductile transition temperature for YSZ films has been estimated ≈800 °C by Morscher G N, Pirouz P and Heuer A H 1991 *J. Am. Ceram. Soc.* **74** 491
[24] Dodson B W 1991 *J. Cryst. Growth* **111** 376
Atkinson A and Jain S C 1992 *J. Appl. Phys.* **72** 2242
[25] Bardal A, Matthée Th, Wecker J and Samwer K 1994 *J. Appl. Phys.* **75** 2902
[26] Thompson C, Palasantzas G, Feng Y P, Sinha S K and Krim J 1994 *Phys. Rev.* B **49** 4902
[27] Tong W M and Williams R S 1994 *Annu. Rev. Phys. Chem.* **45** 401
[28] Wolf D E and Villain J 1990 *Europhys. Lett.* **13** 389
[29] Mullins W W 1957 *J. Appl. Phys.* **28** 333
[30] Frank F C and van der Merwe J H 1949 *Proc. R. Soc.* A **189** 205
[31] Rönnow D, Isidorsson J and Niklasson G A 1996 *Phys. Rev.* E **54** 4021
[32] Movchan B A and Demchishin A V 1969 *Phys. Met. Metallogr.* **28** 83
Thornton J A 1977 *Annu. Rev. Mater. Sci.* **7** 239
Grovenor C R M, Hentzell H T G and Smith D A 1984 *Acta Metall.* **32** 773
[33] Yoon J G, Oh H K and Lee S J 1999 *Phys. Rev.* B **60** 2839
[34] Karl H and Stritzker B 1992 *Phys. Rev. Lett.* **69** 2939
Frey T, Chi C C, Tsuei C C, Shaw T and Boszo F 1994 *Phys. Rev.* B **49** 3483
Dam B, Rector J H, Huijbregtse J M and Griessen R 1998 *Physica* C **305** 1
[35] Dam B, Koeman N J, Rector J H, Stäuble-Pümoun B, Poppe U and Griessen R 1996 *Physica* C **261** 1
[36] Estimated from: Agrawal P M, Rice B M and Thompson D L 2002 *Surf. Sci.* **515** 21
[37] Kasu M and Kobayasin N 1995 *Appl. Phys. Lett.* **67** 2842
DeLuca P M, Labanda J G C and Barnett S A 1999 *Appl. Phys. Lett.* **74** 1719
Slezák J, Ondřejček M, Chvoj Z, Cháb V, Conrad H, Heun S, Schmidt Th, Ressel B and Prince K C 2000 *Phys. Rev.* B **61** 16121
[38] Schlom D G, Anselmetti D, Bednorz J G, Broom R F, Catana A, Frey T, Gerber C H, Güntherodt H-J, Lang H P and Mannhart J 1992 *Z. Phys.* B **86** 163
Stäuble-Pümoun B, Matijasevic V C, Ilge B, Mooij J E, Peterse W J A M, Scholte P M L O, Tuinstra F, Venwik H J, Wai D S, Traeholt C, Wen J G and Zandbergen H W 1995 *Phys. Rev.* B **52** 7604
[39] Chang C C, Wu X D, Inam A, Hwang D M, Venkatesan T, Barboux P and Tarascon J M 1988 *Appl. Phys. Lett.* **53** 517
Izumi H, Ohata K, Sawada T, Morishita T and Tanaka S 1991 *Japan. J. Appl. Phys.* **30** 1956
Jenniches H, Klaua M, Höche H and Kirchner J 1996 *Appl. Phys. Lett.* **69** 3339
[40] Chrisey D B and Hubler G K (ed) 1994 *Pulsed Laser Deposition of Thin Films* (New York: Wiley) chapters 5 and 9
[41] Kindt J T, Tully J C, Head-Gordon M and Gomez M A 1998 *J. Chem. Phys.* **109** 3629
[42] Barth J V 2000 *Surf. Sci. Rep.* **40** 75
[43] Wintterlin J, Schuster R and Ertl G 1996 *Phys. Rev. Lett.* **77** 123
Schmid M, Leonardelli G, Tscheließnig R, Biedermann A and Varga P 2001 *Surf. Sci.* **478** L355
[44] Eltoukhy A H and Greene J E 1980 *J. Appl. Phys.* **51** 4444
Ito A, Machida A and Obara M 1997 *Japan. J. Appl. Phys.* **36** L805
Xu K, Shah S I and Guerin D 2001 *J. Vac. Sci. Technol.* **19** 1078
[45] Sprague J A, Westmore J E, Smidt F A and Malmberg P R 1973 *Trans. Am. Nucl. Soc.* **16** 70
[46] Vasco E 2004 PLD growth kinetics studied through rate-equation approaches, in preparation
[47] Metev S and Meteva K 1989 *Appl. Surf. Sci.* **43** 402
[48] Briner B G, Doering M, Rust H-P and Bradshaw A M 1997 *Science* **278** 257
[49] Sumomogi T, Sakai H, Nakata M and Endo T 1998 *Appl. Phys.* A **66** S815
[50] Koren G, Gupta A, Baseman R J, Lutwycge M I and Laibowitz R B 1989 *Appl. Phys. Lett.* **55** 2450